CoA/ASAE-2

A.S.A.E. REPORT No. 2

LIBRARY

THE COLLEGE OF AERONAUTICS

CRANFIELD

THE ADVANCED SCHOOL OF AUTOMOBILE ENGINEERING

THE EXPERIMENTAL DETERMINATION OF TYRE MODEL PARAMETERS

- by -

J.R. Ellis, F. Frank and B.J. Hinton

1403063695

A.S.A.E. REPORT No. 2

September, 1966

THE ADVANCED SCHOOL OF AUTOMOBILE ENGINEERING
CRANFIELD

CRANFIELD UNIVERSITY LIBRARY

The experimental determination of tyre model parameters

- by -

J.R. Ellis, M.Sc.(Eng.), Ph.D., A.M.I.Mech.E., M.S.A.E.

F. Frank, Dr.Ing.

and

B.J. Hinton, B.Sc., D.Au.E.

SUMMARY

This report describes the analysis of a series of experiments on pneumatic tyres which were designed to test the various hypotheses regarding the deformed shape of a tyre during the steering process.

The experiments consisted of several separate tests first described in Ref. 1 and 2.

a) The application of a point lateral force or a moment at one position on the tread band which is restrained at the centre of the wheel, and the measurement of the resulting lateral deflection of each point of the tyre perimeter.

b) The application of a uniform force around the tyre perimeter on a hollow cylindrical former and applying a load at the centre of the wheel.

c) Direct determination of tread band tension by cutting the tread band and bridging the cut by a dynamometer.

d) Estimation of the bending modulus of the tread band by test on sections cut from the tread band.

The analysis of the experiments is carried out by first transforming the test results into a Fourier series and determining the spectral content of the bending line with an harmonic analysis. Transfer functions of beam and string models are derived and applied to the test results. A method of considering a three parameter model is described.

CONTENTS

1 Introduction

The lateral deflection of the tyre relative to the wheel during cornering is the most significant feature of the mechanism by which a lateral force is generated. In order to provide a starting point for the development of a theory of the cornering power of a tyre several models have been proposed. These tyre models divide the tyre into two distinct parts each with separate properties. The walls of the tyre are assumed to act as a spring attaching the tread band to the wheel rim, while the tread band itself has been variously assumed to act as a taut string, a beam, or a beam under the action of tensile forces.

While this arbitrary division of the tyre into separate regions can be supported by inspection there has been little attempt to justify the selection of a particular model and all the analysis has been made with the object of obtaining lateral force versus angle of steer relationships which can be said to agree with a particular set of test data.

An early attempt to justify the selection of a particular model is given in reference 1. Here tests are described and a theoretical analysis developed of the pneumatic stiffness of the tyre wall and the bending stiffness of the tread band while the lateral deflection of the tread band due to the application of a "point" load in the lateral direction is measured and attempts are made to relate this deflection to the bending stiffness and tension of the tread band. These experiments are continued in reference 2, where, additionally, the tension is measured directly by means of a dynamometer. The present report describes the analysis of the tests made in these references.

Typical bending lines for the laterally load tyres are shown in Fig. 1 and Fig. 2. These tyres have similar overall dimensions, two of the tyres are cross bias construction and two are radial ply.

2 The tyre model

The general model is described by the differential equation:-

$$EId^4y/dx^4 - Td^2y/dx^2 + ky = q(x) \qquad \text{Eq. (1)}$$

EI is the bending stiffness, T is the axial tension and k is the stiffness of the elastic foundation. These parameters are assumed to be constant with respect to x. In the special case where bending stiffness is ignored then the model is referred to as the "taut string" model.

$$- Td^2y/dx^2 + ky = q(x)$$

A typical solution of equation (1) is tedious because the continuity of the tread band requires that end conditions be satisfied and a solution of transcendental form is obtained. The linear dependence of load and deflection has been demonstrated by the experiments of reference 1 and 2 thus it is possible to suggest that analyses of the experiments may be carried out in the transformed domain with the bending lines expressed as a trigonometric series. All the lateral deflections are symmetrical about the load point hence the Fourier series will contain

only cosine terms. Also the requirement of symmetry demonstrates that only derivatives of even order can exist in the mathematical model.

The Fourier coefficients of the bending spectrum $S_y(n)$ which correspond to the deflected shape of the tyre y(x) are obtained by means of an harmonic analyser. Load spectra Sq(n) corresponding to point like load distributions q(x) are derived in Appendix 1, where a discussion on how far a real load distribution may be assumed to be a point load is also given.

The tyre spectrum is defined as:-

$$S_t(n) = S_y(n)/S_q(n) \qquad \text{Eq. (2)}$$

From the experimental data it may be seen that the applied load is, to all intents, a point load, for which all the spectral lines are of constant height.

$$\text{Hence} \qquad S_q(n) = \frac{F}{\pi R_A} \qquad (n = 1, 2, 3 \ldots\ldots\ldots) \qquad \text{Eq. (3a)}$$

except that the average value (n = 0.) is :-

$$S_q(0) = \frac{F}{2\pi R_A} \qquad \text{Eq. (3b)}$$

Fig. 3, 4 are the normalized tyre spectra; the normalized amplitude a_t (n) is defined as:-

$$a_t(n) = S_t(n)/S_{t(0)} \qquad \text{Eq. (4)}$$

$$\text{Where} \qquad S_t(0) = \frac{Sy(0)}{Sq(0)} = R_A \int_0^{2\pi} \frac{Y}{F}\, d\phi \qquad \text{Eq. (5)}$$

Equation (2) defines a tyre spectrum which contains only the characteristics of the tyre itself and is independent of the external loading.

The transfer functions of equation (1) may be obtained by the Laplace transformation.

$$\frac{L(y)}{L(q)} = \frac{1}{EIs^4 - Ts^2 + k} \qquad \text{Eq. (6)}$$

In general s = a + iw. Set a = 0 and give descrete values to w so that the "normalized frequency" is a multiple of the tyre perimeter.

$$w = 2\pi.n.\ \frac{1}{2\pi R_A} = n/R_A \qquad \text{Eq. (7)}$$

Hence the spectrum of equation (6) is :-

$$S_m(n) = \frac{1}{(EI/R_A{}^4)n^4 + (N/R_A{}^2)n^2 + k} \qquad \text{Eq. (8)}$$

$$\text{or} \quad a_m(n) = \frac{1}{A_{4.0}n^4 + A_{2,0}n^2 + 1} \qquad \text{Eq. (9)}$$

$$\text{where } a_m(n) = S_m(n)/S_m(0) = K.S_m(n) \qquad \text{Eq. (10)}$$

The constants are defined as:-

$$A_{4.0} = EI/R R_A{}^4 \quad . \quad A_{2.0} = T/R R_A{}^2 \qquad \text{Eq. (11)}$$

Consider the 'beam' model, then as n tends to infinity we have:-

$$\lim_{n \to \infty} a_m(n) = \frac{1}{A_{4.0}n^4} \qquad \text{Eq. (12a)}$$

or in logarithmic terms,

$$\lim_{n \to \infty} \log a_m(n) = -\log A_{4.0} - 4 \log n. \qquad \text{Eq. (12b)}$$

For the 'taut string' model:-

$$\lim_{n \to \infty} a_m(n) = \frac{1}{A_{2.0}n^2} \qquad \text{Eq. (13a)}$$

$$\text{or} \quad \lim_{n \to \infty} \log a_m(n) = -\log A_{2.0} - 2 \log n. \qquad \text{Eq. (13b)}$$

Hence if the envelope of the spectrum is plotted on log-log paper a 'beam' model will have a slope which tends to 4:1 as n tends to infinity while the 'taut string' model will have a slope of 2:1 in similar circumstances. Examination of Fig. 3, 4, shows that the cross bias tyre is adequately represented by a taut string model, and the radial cord tyre by a beam model.

3 Derivation of model parameters from test data

The tyre spectra of Fig 3 and 4 will now be compared with the spectral curves of a beam and taut string model in order to evaluate the parameters k, $A_{4,0}$ and $A_{2.0}$ so that a best fit is obtained between the deflected shape of the mathematical model $y_m(x)$ and the test data $y(x)$. The most usual conditions will be:-

$$\int_0^{2\pi} (y - y_m)d\phi = 0 \qquad \text{Eq. (14a)}$$

$$(\Delta y)^2 = \frac{1}{2\pi}\int (y - y_m)\, d\phi \rightarrow \text{MIN!} \qquad \text{Eq. (15)}$$

The parameter k may be determined either by the test illustrated in Fig. 1 when,

$$F/_y = 2\pi R_A k \qquad \text{Eq. (16a)}$$

or from integration of the lateral deflection due to a point load, when,

$$1/k = R_A \int_0^{2\pi} F/y.d\phi \qquad \text{Eq. (16b)}$$

Equation (15) states the minimum R.M.S. error condition which, when transformed into the spectral domain results in Parseal's equation.

$$\Delta y = \sqrt{\frac{1}{2\pi}\int_0^{2\pi}(y - y_m)^2 d\phi} = \sqrt{\tfrac{1}{2}\sum_{n=1}^{n=\infty}\left[S_y(n) - S_{y_m}(n)\right]^2} \rightarrow \text{MIN!} \qquad \text{Eq. (17)}$$

Substituting equations (2) and (3a)

$$\Delta y = \frac{F}{2\pi R_A}\sqrt{\tfrac{1}{2}\sum_{n=1}^{\infty}\left[S_t(n) - S_m(n)\right]^2} \rightarrow \text{MIN!} \qquad \text{Eq. (18)}$$

or

$$\frac{\Delta y}{F} = \frac{1}{2\pi R_A k}\sqrt{\sum_{n=1}^{\infty}\left[a_t(n) - a_m(n)\right]^2} \rightarrow \text{MIN!} \qquad \text{Eq. (19)}$$

Equation (9) is a function of the parameters $A_{4.0}$ and $A_{2.0}$ hence simultaneously,

$$\frac{\partial \Delta y}{\partial A_{4.0}} = 0 \quad \text{and} \quad \frac{\partial \Delta y}{\partial A_{2.0}} = 0 \qquad \text{Eq. (20)}$$

also the conditions

$$\frac{\partial^2 \Delta y}{\partial A_{4.0}^2} > 0. \quad \frac{\partial^2 \Delta y}{\partial A_{2.0}^2} > 0. \quad \frac{\partial^2 \Delta y}{\partial A_{4.0}^2}\cdot\frac{\partial^2 \Delta y}{\partial A_{2.0}} - \frac{\partial^2 \Delta y}{\partial A_{4.0}\partial A_{2.0}} > 0.$$

are sufficient to ensure that y is a mimimum. Differentiating equation (19) with respect to the parameters defined in equation (9) leads to two simultaneous conditions for $A_{4.0}$ and $A_{2.0}$:

$$\sum_{n=1}^{\infty}\left[a_t(n) - a_m(n)\right]\left[na_m(n)\right]^2 = 0$$

$$\sum_{n=1}^{\infty}\left[a_t(n) - a_m(n)\right]\left[n^2 a_m(n)\right]^2 = 0 \qquad \text{Eq. (22)}$$

Where $a_t(n)$ are the measured normalized tyre spectral amplitudes and $a_m(n)$ are the model amplitudes.

It will be assumed that the conditions of equations (21) are satisfied and no check calculation is offered.

In order to arrive at some simple conclusions it will be initially assumed that either one parameter or the other dominates the deflection spectrum.

Cross bias tyres $$a_m(n) = \frac{1}{A_2 n^2 + 1}$$ Eq. (23a)

Radial cord tyres $$a_m(n) = \frac{1}{A_4 n^4 + 1}$$ Eq. (23b)

Where A_4 and A_2 replace $A_{4.0}$ and $A_{2.0}$ respectively.
Then a single condition replaces equations (22)

$$\sum_{n=1}^{m} \left[a_t(n) - \frac{1}{A_2 n^2 + 1} \right] \left[\frac{n}{A_2 n^2 + 1} \right] = 0$$ Eq. (24a)

$$\sum_{n=1}^{m} \left[a_t(n) - \frac{1}{A_4 n^4 + 1} \right] \left[\frac{n}{A_4 n^4 + 1} \right] = 0$$ Eq. (24b)

For practical analysis the series must be finite and in view of the limited accuracy of the experimental data only a few terms need be considered. m = 6 is a reasonable limit and it can be shown by digital computation that this produces errors less than 0.5% in A_4 or A_2.

Further approximations are now made.

$$\left.\begin{aligned} \frac{1}{A_2 n^2 + 1} &\simeq \frac{1}{A_2 n^2} \\ \frac{1}{A_4 n^4 + 1} &\simeq \frac{1}{A_4 n^4} \end{aligned}\right\} \quad n > m.$$

Equations (19) now take the form:-

$$\Delta y/F = \frac{1}{\sqrt{2\pi R_A k}} \cdot \sqrt{\sum_{n=1}^{m} \left[a_t(n) - a_m(n) \right]^2 + \frac{1}{A_2^2} \sum_{n=m+1}^{\infty} 1/n^4}$$ Eq. (26a)

$$\Delta y/_F = \frac{1}{\sqrt{2\pi} R_A k} \sqrt{\sum_{n=1}^{m} \left[a_t(n) - a_m(n) \right]^2 + \frac{1}{A_4^2} \sum_{n=m+1}^{\infty} 1/n^8} \qquad \text{Eq. (26b)}$$

The values of A_2 and A_4 are found from an iterative procedure which starts from the determination of the upper and lower boundaries for these parameters and continues until condition (24a,b) is satisfied. Figs. 5,6,7,8 show the results. All parameters depend on inflation pressure. From this it is concluded that the parameter EI is dominant for radial cord tyre, whereas T is the major parameter for cross bias tyres. The pneumatic stiffness k has a content due to the stiffness of the tyre construction and will be dependent on the tyre shape as demonstrated in reference 1.

4 Three parameter models

Equation (1) shows a tyre model dependent on both bending stiffness and tread band tension and so far the condition for either bending stiffness or tension has been considered with the inference that in the one case tension is unimportant, and in the other case that no bending stiffness exists.

The next step is, therefore, to separate the bending and tension terms. It is known from reference 2, that direct measurement of the tread band tension is possible and the experiment indicates that T is a linear function of inflation pressure. Consider T_{p_o} as a "standard" tension related to a pressure p_o, therefore at any other pressure.

$$T = \frac{p}{p_o} (T_{p_o}) \qquad \text{Eq. (27)}$$

also assume EI = constant.

In this analysis the curves A_4 = constant Fig. 12 were plotted for six inflation pressures, but the ordinate is multiplied by $K.R_A^4$, hence, from equation 11, the diagram Fig. 9 then shows EI as a function of inflation pressure and $A_{2.0}$. This parameter, $A_{2.0}$ is given by equations (11) and (27) and its development is shown in the lower part of Fig. 13. T_{p_o} is the slope of the straight line in the lower right quadrant and this is found by trial and error to suit the condition EI = constant. Different functions EI = f(p.T_{p_o}) are plotted in the upper left quadrant of Fig. 9. The condition EI = constant is satisfied for the two tyres considered if the following values of T_{p_o} and EI are used.

Tyre

D. 6.50 - 16 RB $\quad T_{p_o} = 220\text{kp}$, $EI = 205000\text{kp cm}^2$

M. 6.00 - 16 X $\quad T_{p_o} = 210\text{kp}$, $EI = 150000\text{kp cm}^2$

The model spectra and tyre spectra are now compared for one tyre.

Tyre M. 6.00 - 16 X $p = 2.5$ kp/cm^2

n	1	2	3	4	5	6
$a_t(n)$	.895	.296	.056	.0189	.009	.0008
$a_m(n)$	.772	.349	.1292	.0517	.024	.012
$a_t - a_m$	+ .123	- .053	- .0732	- .0328	- .015	- .0102

It will be noted that the first harmonic of the tyre bending spectrum is considerably greater than given by the spectral form of equation (1). This discrepancy is difficult to explain except by assuming that a hoop like deformation occurs in which the tread band tilts on the side walls.

A direction comparison of tread band tension obtained from this analysis with experimental data obtained in an experiment in which the tread band was cut and then held in position by a dynanometer gives the following results:

6.00 - 16 Tyre	Bending line analysis	$T_{p_o} = 210$ kp
	Experiment	$T_{p_o} = 193$ kp

5 Conclusions

An analysis of the experimental bending line measurements by spectral techniques suggests that the dominant terms in the tyre model of equation (1) are:-

For a radial cord tyre - bending stiffness.
For a cross bias tyre - tread band tension

a) Pneumatic stiffness

The experimental measurements predict that the pneumatic stiffness is a function of inflation pressure and indicate the presence of a residual stiffness in the tyre walls. Reference 1 predicts that the pneumatic stiffness is also a function of the tyre profile, unfortunately it has not been possible to test the hypothesis since all the tyres available are of approximately similar cross section.

b) Tread band tension

Analysis of the measured bending lines indicates that the tread band tension is the dominant term in the tyre model when this is applied to cross bias tyres. Reasonable agreement is obtained between the measured value of tension and that obtained from a curve fitting technique.

c) Bending stiffness

Values of EI of 205000 kp cm^2 for a 6.50 - 16 radial cord tyre and 150000 kp cm^2 for a 6.00 - 16 radial cord tyre are in reasonable agreement with tests described in reference 1 in which a section removed from the tread band of a

similar tyre gave a value of E = 11,400 kp/cm^2 and a bending stiffness on a section 1.9 cm in the direction of bending of EI = 650 kp cm^2.

No analysis is presented for fabric cord tyres but the values of E and EI as measured on a test section are, from reference 1, E = 70 kp/cm^2 and with a test section 2.06 cm in the direction of bending. EI = 97 kp cm^2.

d) General

The method of analysis demonstrated here would appear to be a suitable method of estimating the parameters of the tyre model used previously, without justification, by a number of authors.

Satisfactory agreement has been demonstrated for a limited number of tests and analyses.

REFERENCES

1 ELLIS, J.R. Ph.D. Thesis, University of London (1960).

2 HINTON, B.J. Investigation of tread band deformation under point lateral load. Diploma Thesis No 61/2, Advanced School of Automobile Engineering, Cranfield, Bedfordshire (England) (1961).

3 FRANK, F. Theorie des Reifenschraglaufs. Dr - Ing. Thesis Technische Hochschule, Darmstadt. (1965).

4 BIDERMAN, V.L. Tyres with Transverse Carcass Cords. Soviet Rubber Technology, 20(1960), No 7, p. 10 - 12.

5 BOECKH, Ermittlung der elastischen Konstanten von Flugzeugreifen. Report FW - WVA - 13-3703, Dez. 1944, Focke Wulf Flugzeugbau GmbH, Bremen and: NACA TM 1378(1954) (Engl. translation).

6 BORGMANN, W. Theoretische und experimentelle Untersuchungen an Luftreifen bei Schräglauf. (Theoretical and experimental investigations on cornering tyres). Dissertation Technische Hochschule Braunschweig, 1963 (Germany) 120 pages.

7 COOPER, D.H. Die Verteilung der Seitenführungskraft und des Schlupfes in der Bodenberührungsfläche von Reifen. Kautschuk und Gummi 11(1958), No. 10, p. WT 273 - 277, and: Automobile Engineer 48(1958), No 13, p. 524, and: Revue generale du Caoutchouc 36(1959) No 10, p. 1331, and: ATZ(1961) No 2, p. 51 - 56.

8 DOETSCH, G. Einführung in die Theorie der Laplace-Transformation. Birkhauser Verlag, Basel 1958, 301 pages.

9 FIALA, F. Seitenkräfte am rollenden Luftreifen. (Cornering forces of rolling tyres). VDI-Zeitschrift 96(1954), No 29, p. 973 - 979.

10 FREUDENSTEIN, G. Luftreifen bei Schräg- und Kurvenlauf. (Pneumatic tyres when running at an angle or on curves). Deutsche Kraftfahrzeugforschung und Strassenverkehrstechnik, No 152(1961), 56 pages.

11 ELLIS, J.R. and FRANK, F. A.S.A.E. Report No. 1.

12 GOUGH, V.E. Nondestructive estimation of resistance of tyre construction to tread wear. SAE preprint 667 A (1963).

13 HETENYI, M. Beams on elastic foundation. University of Michigan Press 1953.

14 HILDEBRAND, F.B. Introduction to Numerical Analysis. McGraw-Hill Book Comp. 1956, 511 pages.

15 HORNE, W.B. SMILEY, R.F. STEPHENSON, B.H. Low-Speed Yawed-Rolling Characteristics and other Elastic Properties of a Pair of 26-inch-Diameter 12-Ply-Rating Type VII Aircraft Tires. NACA Technical Note No 3604 (1956).

16 MEYER zur CAPELLEN, W. Mathematische Instrumente. Leipzig 1944.

17 RYSHIK, I.M. GRADSTEIN, I.S. Tables of series, products and integrals VEB Deutscher Verlag der Wissenschaften Berlin 1963 (2nd edition) (Translation of the Russian edition - 1951). 438 pages.

18 STEVENS, J.E. Relaxation characteristics of pneumatic tires. Journal of the Aero-Space Sciences 26(1959), p. 340 - 350.

19 THORSON, H.R. A rational method for predicting tire cornering forces and lateral stiffness. Boeing Airplane Co. Report No D-11719 (1951), 39 pages.

20 WILLERS, F.A. Mathematische Instrumente. Oldenbourg Verlag München 1943.

Appendix 1: Spectra of Quasi Point Loads

Table AI.1 shows a collection of symmetric loading functions and the corresponding spectra, and for discussion, the asymptotic behaviour of the envelope of the spectrum, the so called corner frequency n_c, the amount of the envelope at this point, and its difference from unity are included.

Definitions:

1. Total loading force $$F = \int_0^{2\pi R_A} q(x)dx \qquad (AI.1)$$

3. The corner frequency of the envelope is obtained from the intersection of $2q(o)$ and $q(x)$ $n \to \infty$

   i.e. from $$2q(o) = \underset{n \to \infty}{q(x)} \qquad (AI.2)$$

In this case n is assumed continuous.

From table AI.1 it can be seen that the diminution of the envelope at the corner frequency is related directly to the smoothness of the transient of the loading function q(x).

If we assume that the amount of the 8th harmonic of a tyre spectrum is less than one percent of the 1st harmonic but the corner frequency should be higher than the number of the above harmonic then we may estimate the width $2\phi_L$ of a loading function which is just permissible as an approximation of a distributed load by a point load. Reversing the expression for the corner frequency in table 1 we have

$$\phi_L = \frac{1}{n_c} = \frac{1}{8} = 7{,}15^o$$

If the tyre radius is about R_A = 32 cm as in the case of the tyres tested then the maximum permissible loading width is

$$2\phi_L 2\pi R_A = 8\text{cm} \qquad (AI.4)$$

Analogous to this estimation an estimation of the effect of the hump very close to the point of load application can be made (Fig. AI.1)

Appendix II. Effect of the "Third Parameter"

It is the purpose of this Appendix to enable a separation of a non-dominating "third" parameter from a determined effective parameter of a two-parameter model. This will be performed by determination of a function which expresses the effective parameter of a two-parameter model in terms of given dominating and non-dominating parameters of a three-parameter model. The inverse of this function is the solution required.

By normalized notation the numbers of parameters are reduced by one supposing that both models have equal parameters K. Due to the condition of minimum RMS-error between bending lines of these two models we have to satisfy the following equation for a string like model,

$$\sum_{n=o}^{\infty}\left(\frac{1}{A_{40}n^4 + A_{20}n^2 + 1} - \frac{1}{A_2 n^2 + 1}\right)\left(\frac{n}{A_2 n^2 + 1}\right)^2 = 0$$

and for a beam-like model

$$\sum_{n=o}^{\infty}\left(\frac{1}{A_{40}n^4 + A_{20}n^2 + 1} - \frac{1}{A_4 n^4 + 1}\right)\left(\frac{n^2}{A_4 n^4 + 1}\right)^2 = 0$$

These equations were derived in Sect. 3 (see appropriate conditions given by equation (24a, b).

The functions $A_2 = f(A_{20}, A_{40})$ and $A_4 = f(A_{40}, A_{20})$ were computed in an iterative precedure as mentioned in Sect 3,, and they are plotted in Figs. (AII.1) and (AII.2). From these the inverse functions $A_{20} = f(A_2, A_{40})$ and $A_{40} = f(A_4, A_{20})$ were obtained by graphical means. Figs. AII.3 and AII.4 show the required inverse functions and a family of curves for constant amounts of $2\,\frac{\sqrt{A_{40}}}{A_{20}}$.

Appendix III. Slope of Spectrum Envelope

In Sect 2 the spectrum of a beam model in normalized notation was derived as

$$a_m(n) = \frac{1}{A_{40}n^4 + A_{20}n^2 + 1} \qquad \text{(AIII.1)}$$

Considering now the envelope of this spectrum we put n as continuous and using the abbreviation $\eta = n^4 \cdot \sqrt{A_{40}}$ we obtain

$$a_m(\eta) = \frac{1}{\eta^4 + \frac{A_{20}}{\sqrt{A_{40}}}\eta^2 + 1} \qquad \text{(AIII.2)}$$

and in logarithmic representation as shown in Fig (AIII.1), we have

$$\lg a_m(\eta) = -\lg\left(\eta^4 + \frac{A_{20}}{\sqrt{A_{40}}}\eta^2 + 1\right) \qquad \text{(AIII.3)}$$

The slope of the envelope on such a log-log plot is

$$\frac{d\lg a_m}{d\lg \eta} = \eta \cdot \frac{d\lg a_m}{d\eta} \qquad \text{(AIII.4)}$$

Applied to equation (AIII.3) and with use of equation (AII.2) we have

$$\frac{d\lg a_m}{d\lg \eta} = -4\left[1 - a_m(\eta)\left(\frac{A_{20}}{2\sqrt{A_{40}}}\eta^2 + 1\right)\right] \qquad \text{(AIII.5)}$$

and equation (AIII.2) solved for η^2 yields

$$\eta 2 = -\frac{A_{20}}{2\sqrt{A_{40}}} - \sqrt{\frac{A^2_{20}}{4A_{40}} - \left(1 - \frac{1}{a_m}\right)} \qquad \text{(AIII.6)}$$

By substitution of this expression into equation (AIII.5) the final result

$$\frac{d\lg a_m}{d\lg \eta} = -4\left[c - \frac{A_{20}}{2\sqrt{A_{40}}} \cdot \sqrt{c.a_m}\right] \qquad \text{(AIII.7)}$$

where

$$c = 1 + a_m\left(\frac{A^2_{20}}{4A_{40}} - 1\right)$$

From this it follows that at a given amplitude a_m the slope of a spectrum envelope plotted on log-log paper is only dependent on the ratio $2\frac{\sqrt{A_{40}}}{A_{20}}$. This fact may be used for determination of this ratio from a given log-log plot of a beam-like spectrum. For this purpose the curves corresponding to equation (AIII.7) were plotted in Fig. AIII.2.

Appendix IV: Calculation of Tread Band Tension.

The following calculation will be made under the assumption that the cross section of the tread band is a circular arc and that the tread band itself is rigid. If the sidewalls are cut from the tread band and the latter is cut in two opposite sections as shown in Fig (AIV.1) then the equilibrium condition for the remaining annulus is

$$2N = pA_G - 2\int_0^{\pi} N_{\theta G}\cos\theta_G \sin\phi \, d\phi \qquad \text{(AIV.1)}$$

where p is the inflation pressure and the other symbols are explained by Fig (AIV.1). The shaded area is

$$A_G = 4G(R_A - R_{1G}) + 2GR_{1G}\sin\theta_G + 2R^2_{1G}\left(\frac{\pi}{2} - \theta_G\right) \qquad \text{(AIV.2)}$$

Substituting $R_{1G} = \frac{G}{\cos\theta_G}$

We obtain

$$A_G = 4R_A G - 2G^2 \frac{2 - \sin\theta_G - \frac{\frac{\pi}{2} - \theta G}{\cos\theta G}}{\cos\theta_G} \qquad \text{(AIV.3)}$$

After the integration of the second term of equation (AIV.1) is carried out we have to substitute the following expressions from A.S.A.E. Report No. 1.

$$N_\theta^1 = p \frac{R_A^{12} - r_b^2}{2r} \qquad \text{(AIV.4)}$$

$$R_A{}^1 - A^1 = R_A - A \qquad \text{(AIV.5)}$$

and

$$A^1 = R_A{}^1 - r_b \qquad \text{(AIV.6)}$$

which yields

$$2\int_0^{\pi} N_{\theta G}\cos\theta_G \sin\phi r_G d\phi = 2pA^1\left(2(R_A - A) + A^1\right)\cos\theta_G \qquad \text{(AIV,7)}$$

Combining now equation (AIV.3) and equation (AIV.7) we obtain the result

$$N = p\left[2R_A(G - A^1\cos\theta_G) + A^1(2A - A)^1\cos\theta_G - G^2 \frac{2 - \sin\theta_G - \frac{\frac{\pi}{2} - \theta G}{\cos\theta G}}{\cos\theta_G}\right]$$

(AIV. 8)

where from A.S.A.E. Report No. 1.

$$A^1 = \frac{1}{\sin\theta_G}\left(A - G\frac{1 - \sin\theta_G}{\cos\theta_G}\right) \qquad \text{(AIV,9)}$$

Example:

A tyre similar to the measured M6.00-16X of same manufacture was given as an example in above mentioned report of the author. Its geometrical data were:

cross section height:	A = 55 mm
cross section width:	2B = 150 mm
tread band width:	2G = 120 mm

from this data the angle $\theta_G = 50^o$ was computed. Taking now into account the radius, which is R_A = 320 mm, the tread band tension may be computed by use of equations (AIV.8, 9). At p = 1 kp cm^{-2} the result is

N = 214 kp.

Reference should be made to a paper by BIDERMAN (1960).

Appendix V: Hoop on Elastic Foundation

A point load F acting on a rigid hoop on elastic foundation as shown in Fig (AIV.1) may be made up from two parallel forces each of magnitude $\frac{1}{2}F$ and from a couple $R_A.F$, where R_A is the radius of the hoop. The parallel forces mentioned above give rise to the average of the deflection line

$$Y_{no} = \frac{F}{k2\pi R_A} \tag{AV.1}$$

where k is the modulus of elastic foundation. The equilibrium condition with respect to the couple is, for small deflections,

$$R_A F = 4 \int_0^{\frac{\pi}{2}} k Y_{n1}(\phi) R_A \cos\phi \, d\phi$$

and the deflection line is cosine-shaped

$$Y_{n1}(\phi) = Y_{n1max} \cos\phi \tag{AV.3}$$

Substituting this in the above integral and integrating we obtain

$$Y_{n1max} = \frac{F}{k\pi R_A} \tag{AV.4}$$

Combination of equations (AV. 1,3,3) yields the deflection line of the hoop

$$Y_n = \frac{F}{k2\pi R_A} (1 + 2\cos\phi) \tag{AV.5}$$

which is shown in Fig (AV.2). The corresponding bending spectrum simply is

$$\begin{aligned} s_y(o) &= \frac{F}{k \cdot 2\pi R_A} \\ s_y(1) &= \frac{F}{k\pi R_A} \end{aligned} \tag{AV.6}$$

Referring to equation (3a, b) of Sect 2 the hoop spectrum is

$$s_n(o) = s_n(1) = \frac{1}{k} \tag{V.7}$$

i.e. there are only two spectral lines of constant height equal to the inverse of the modulus of elastic foundation.

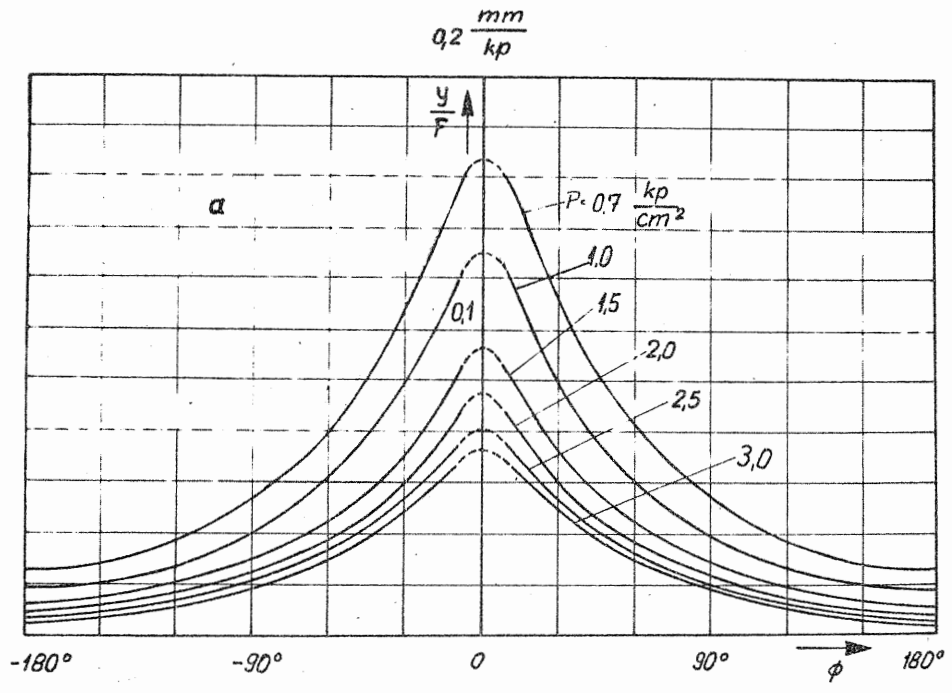

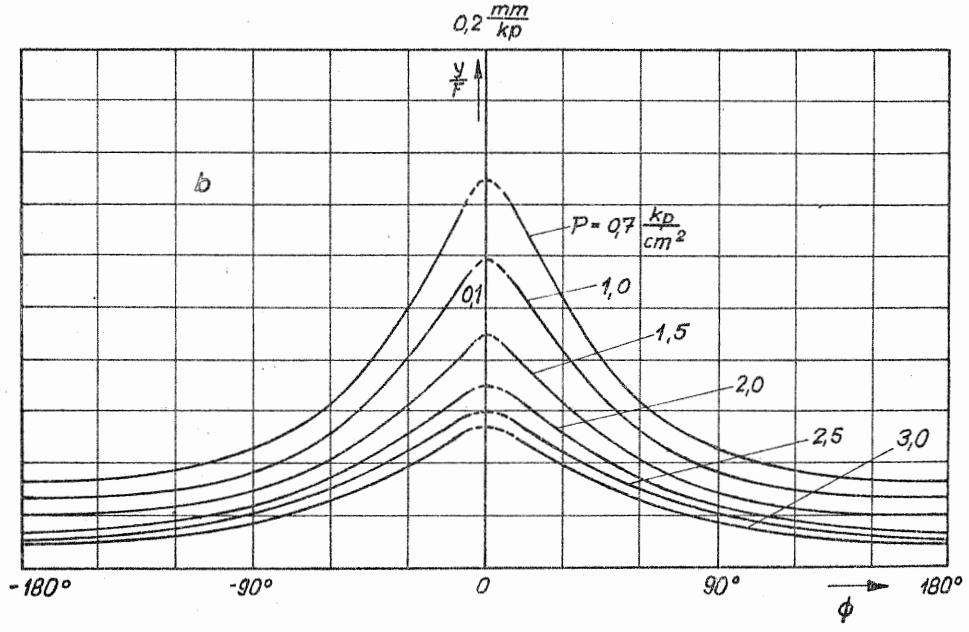

FIG. 1 BENDING LINES OF CROSS BIASED TYRES AT VARIOUS DEFLATION PRESSURES.

a. tyre D6. 70 - 16 b. tyre M6. 00 - 16
(Because of dashed lines at $\phi = 0$ see Fig. AI. 1)

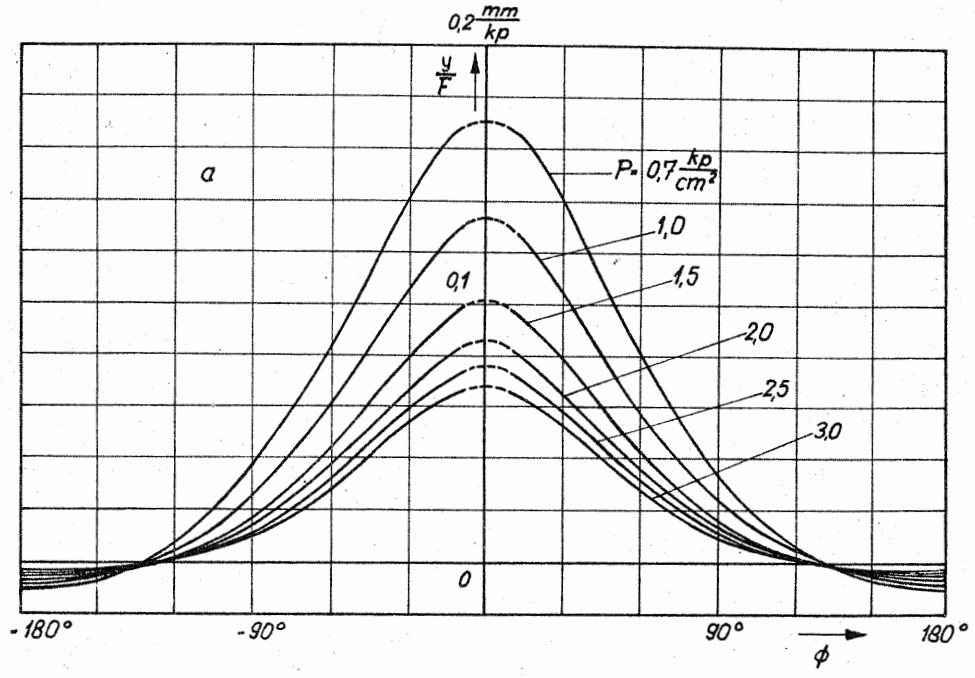

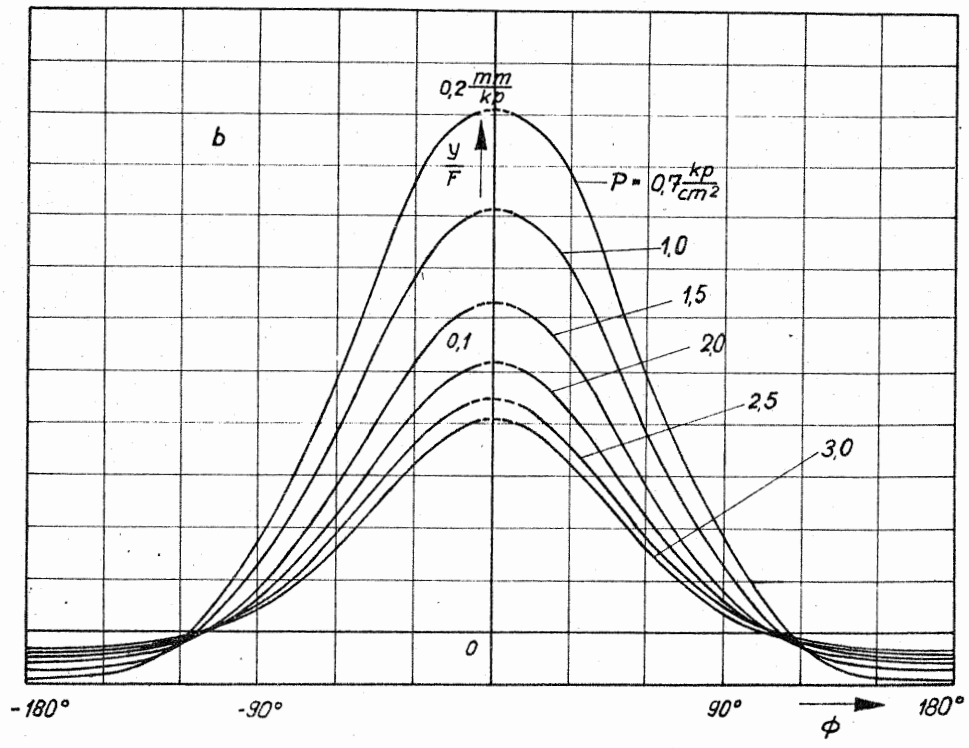

FIG. 2 BENDING LINES OF RADIAL CORD TYRES AT VARIOUS INFLATION PRESSURES p

a. tyre D6. 50 - 16RB b. tyre M6. 00 - 16X
(Because of dashed lines at $\phi = 0$ see Fig. AI. 1)

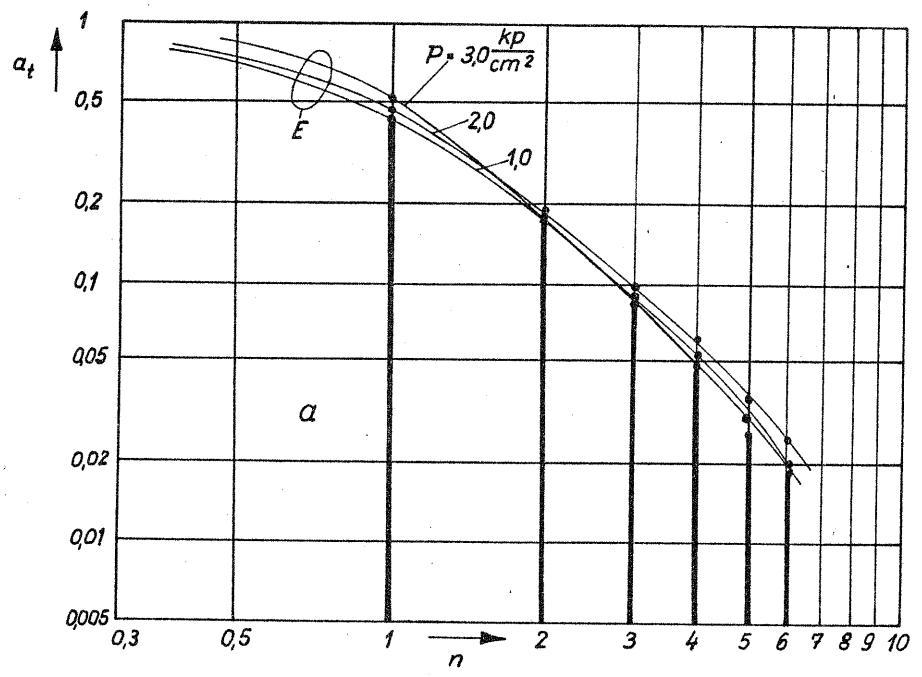

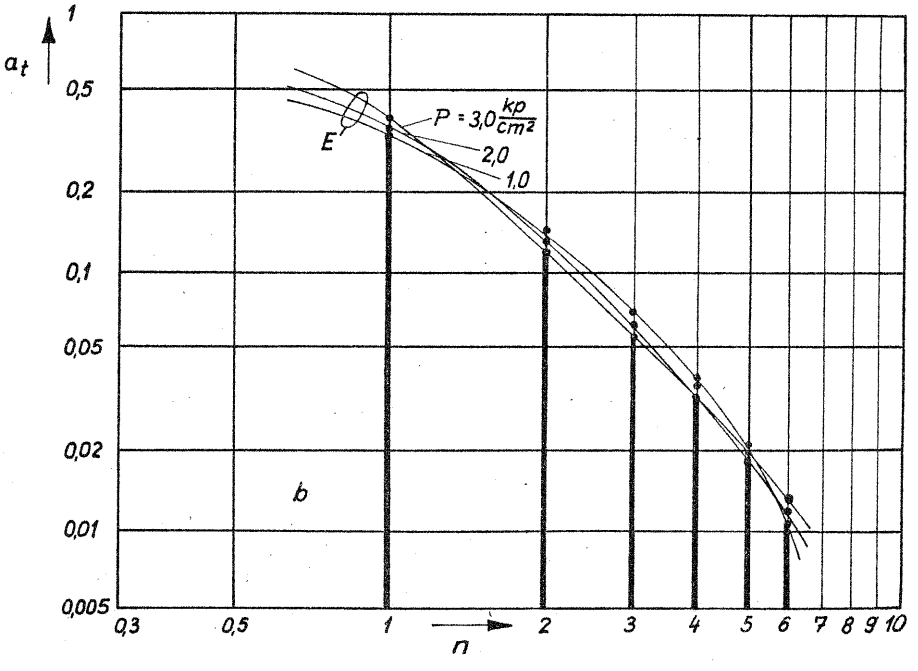

FIG. 3 NORMALIZED TYRE SPECTRA OF CROSS BIASED TYRES AT VARIOUS INFLATION PRESSURES p (E = ENVELOPE OF SPECTRUM)

a. tyre D6. 70 - 16 b. tyre M6. 00 - 16

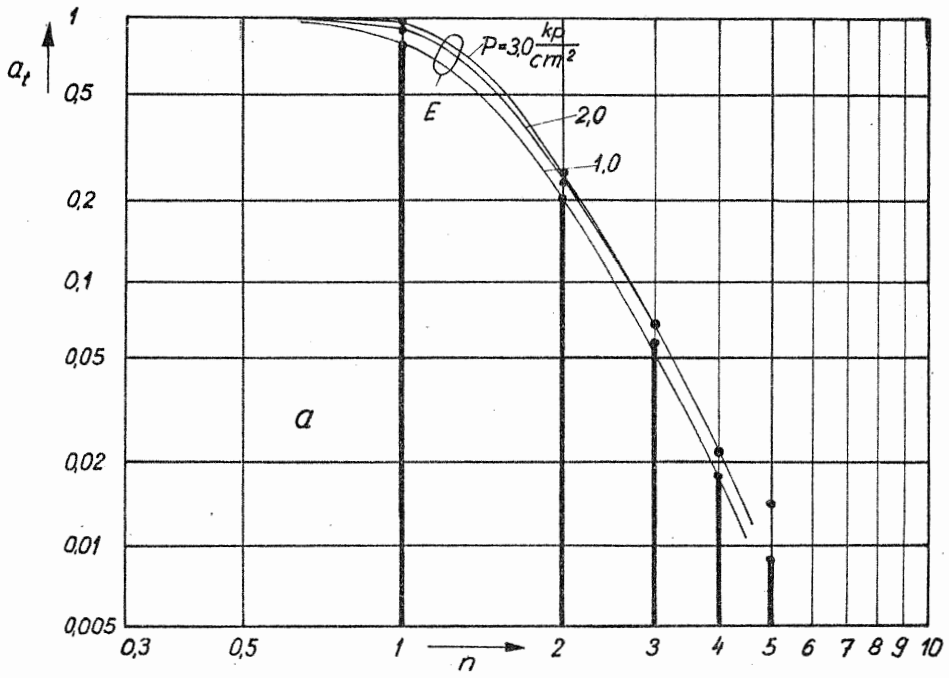

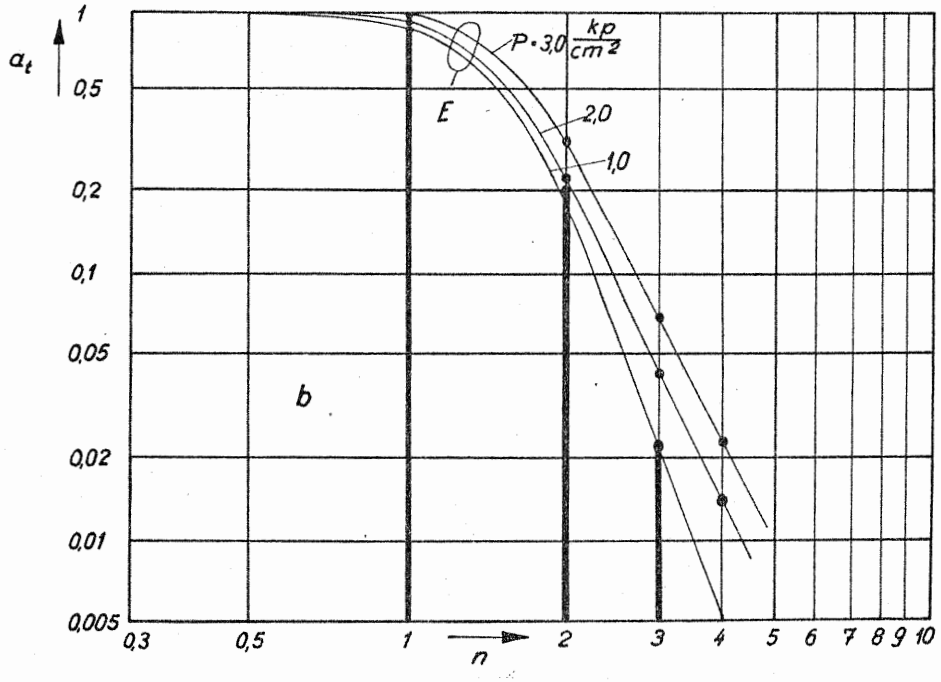

FIG. 4 NORMALIZED TYRE SPECTRA OF RADIAL CORD TYRES AT VARIOUS INFLATION PRESSURES p (E = ENVELOPE OF SPECTRUM)

a. tyre D6.50 - 16RB b. tyre M6.00 - 16X

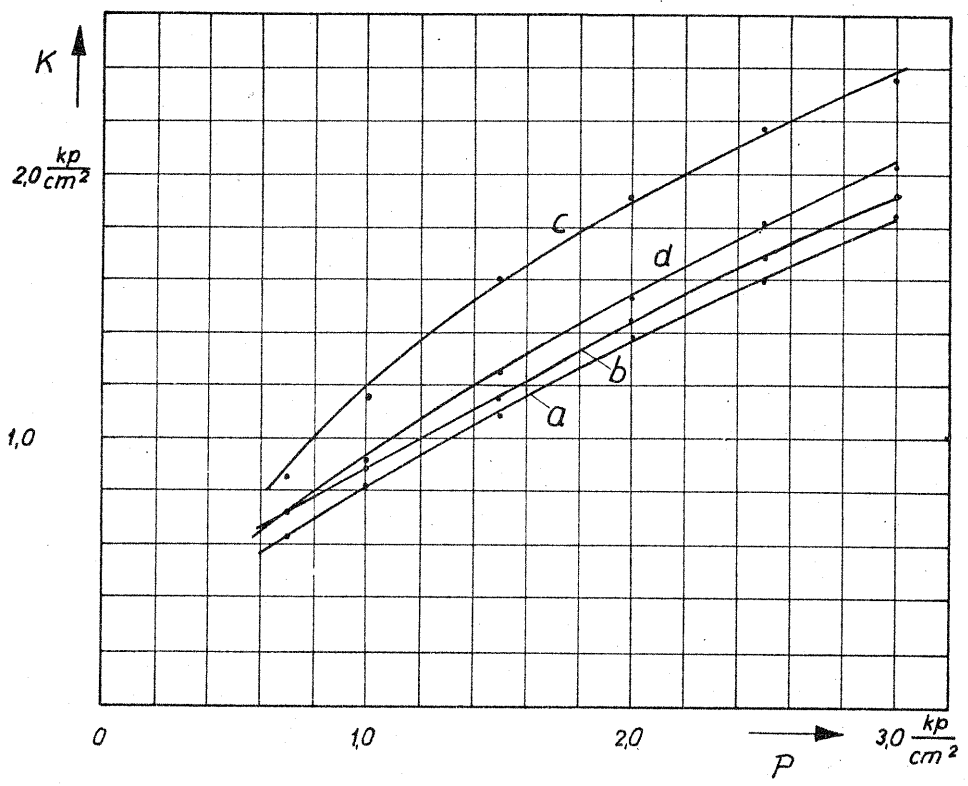

FIG. 5 MODEL PARAMETER k = k(p)

a. tyre D6. 70 - 16
b. tyre M6. 00 - 16
c. tyre D6. 50 - 16RB
d. tyre M6. 00 - 16X

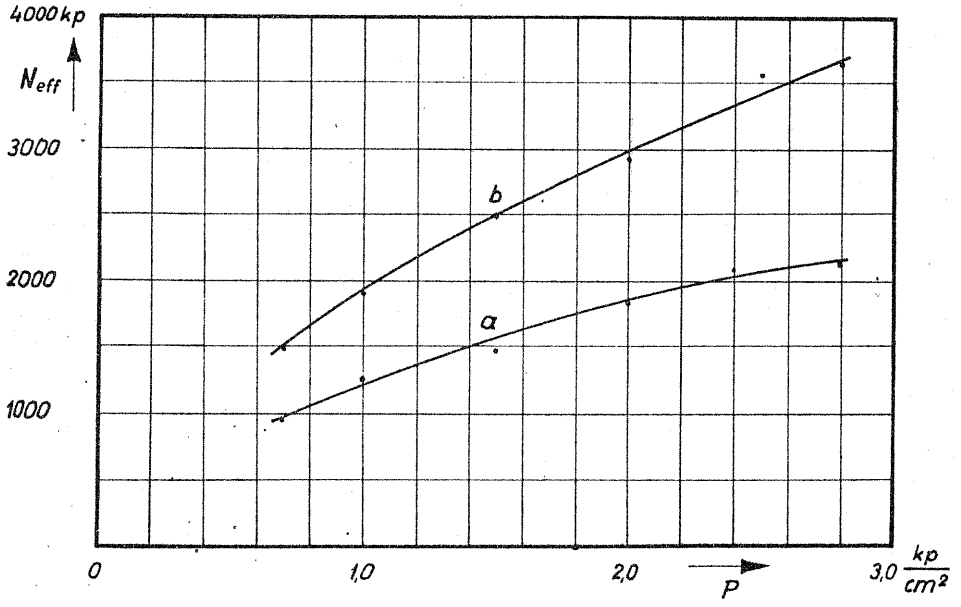

FIG. 6 MODEL PARAMETER $N_{eff} = N_{eff}(p)$ OF CROSS BIASED TYRES

a. tyre D6. 70 - 16
b. tyre M6. 00 - 16

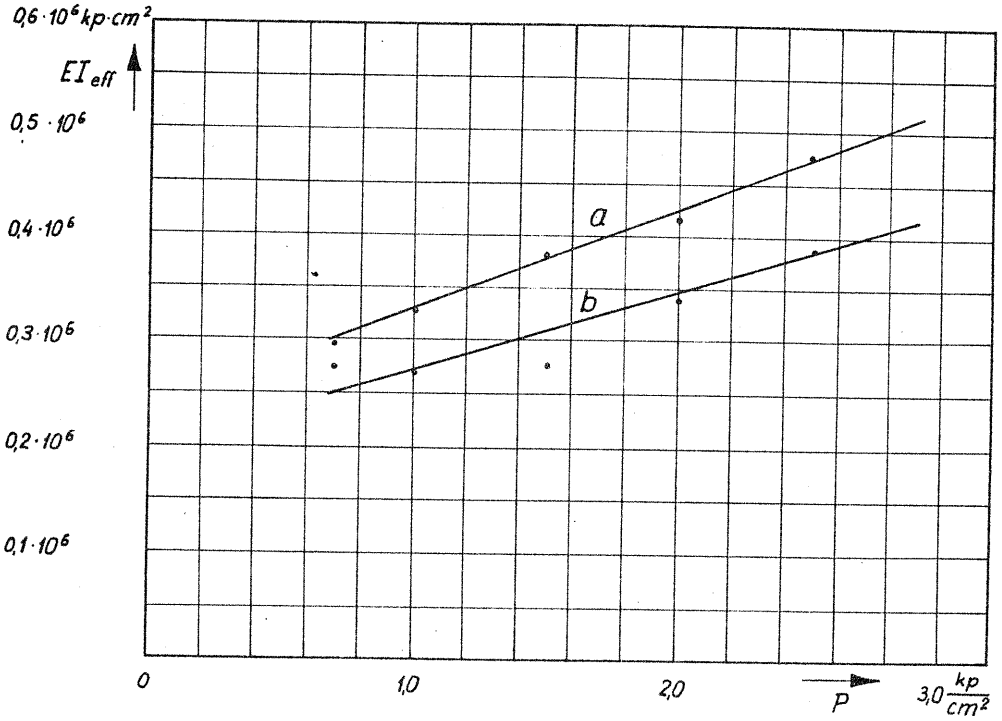

FIG. 7 MODEL PARAMETER $EI_{eff} = EI_{eff}(p)$ OF RADIAL CORD TYRES
a. tyre D6. 50 - 16RB b. tyre M6. 00 - 16X

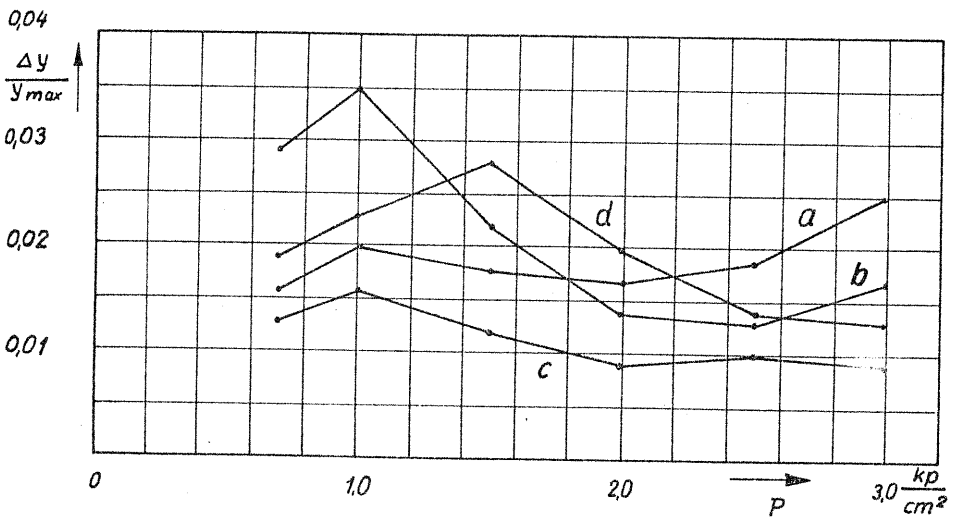

FIG. 8 RMS - ERRORS $\frac{y}{y_{max}}$ OF MODEL BENDING LINES

a. tyre D6. 70 - 16 b. tyre M6. 00 - 16
c. tyre D6. 50 - 16RB d. tyre M6. 00 - 16X

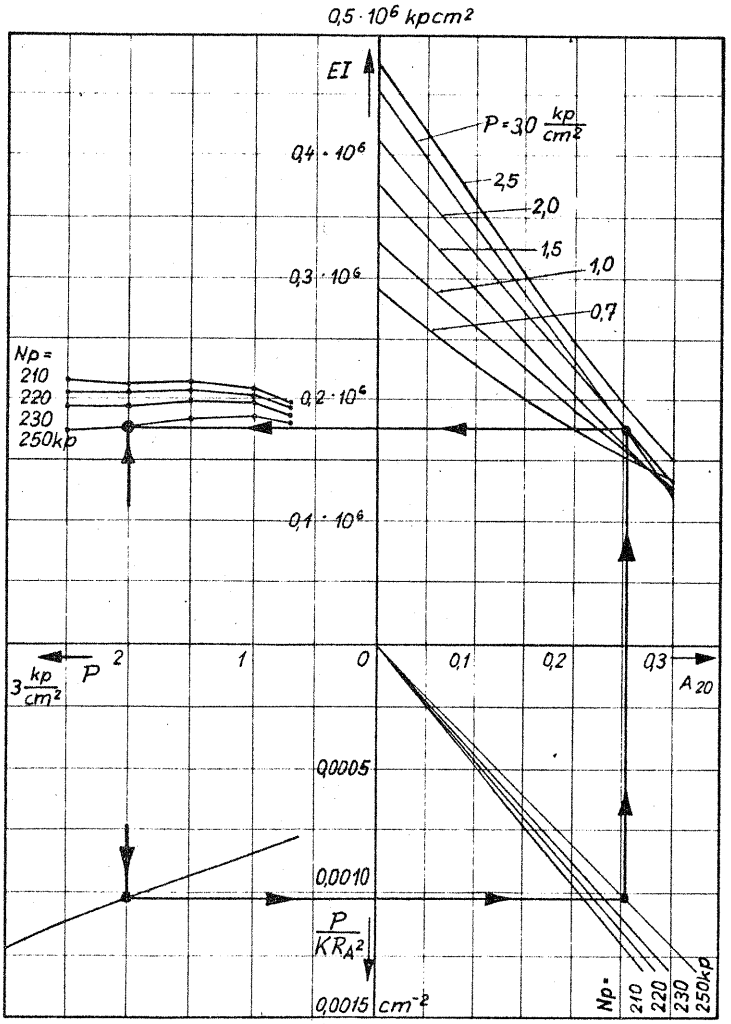

FIG. 9 SEPARATION OF PARAMETER $N = \frac{p}{p_o} N_p$ FROM THE EFFECTIVE PARAMETER EI_{eff} (example chosen: tyre D6. 50 - 16RB)

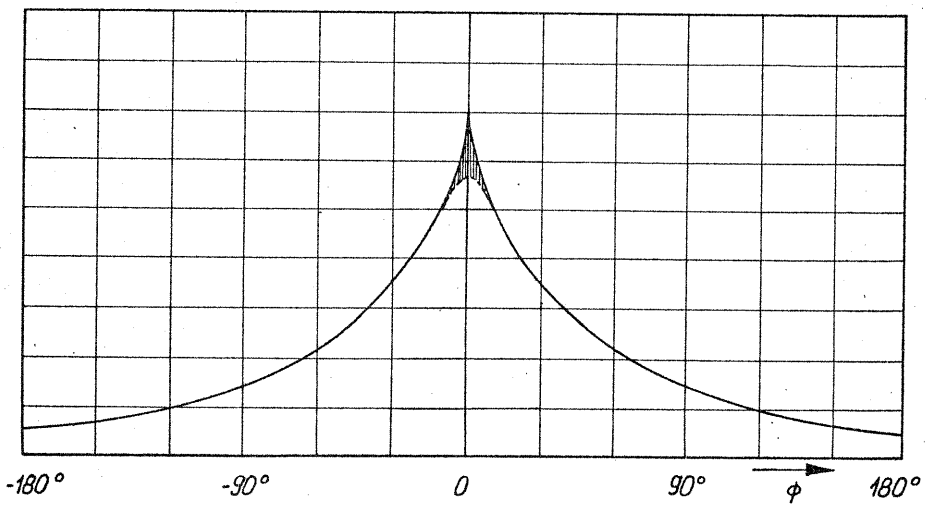

FIG. AI. 1 HUMP ON BENDING LINE (S SHADED) DUE TO STRESS CONCENTRATION CLOSE TO THE POINT OF LOAD APPLICATION (ϕ = 0) (EXAMPLE CHOSEN: TYRE D6. 70 - 16, $p = 1,5 \frac{kp}{cm^2}$)

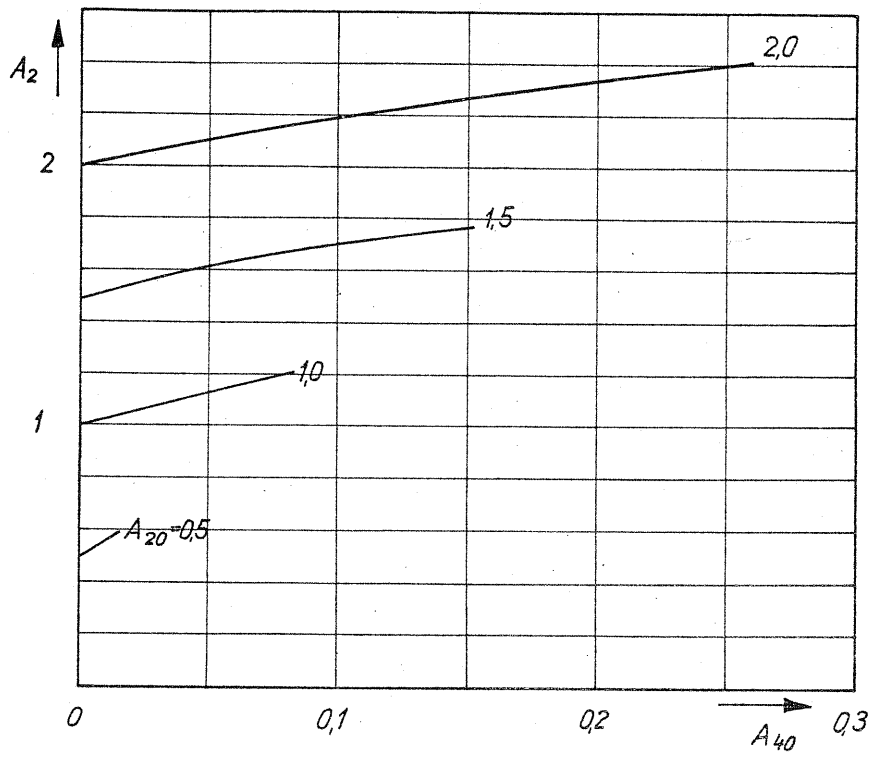

FIG. AII. 1 EFFECTIVE PARAMETER OF A_2 AS A FUNCTION OF THE PARAMETERS A_{20}, A_{40} OF A THREE-PARAMETER MODEL

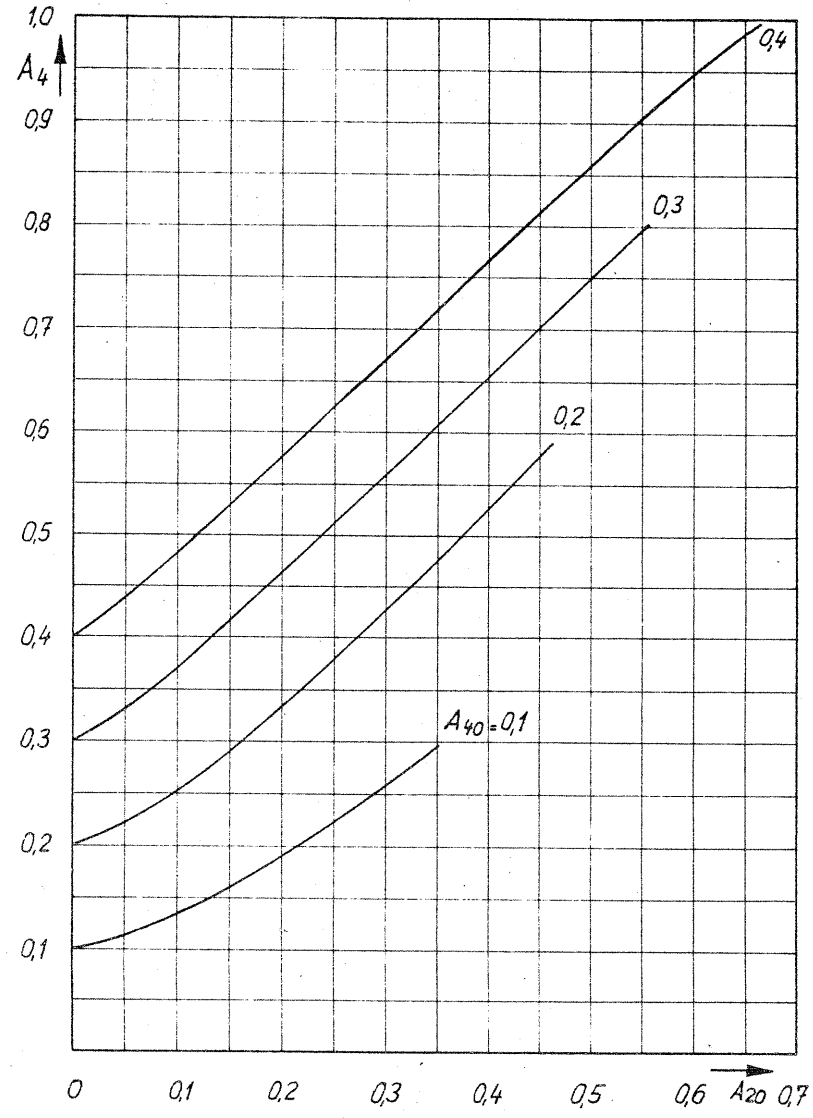

FIG. AII. 2 EFFECTIVE PARAMETER A_4 AS A FUNCTION OF THE PARAMETERS A_{20}, A_{40} OF A THREE-PARAMETER MODEL.

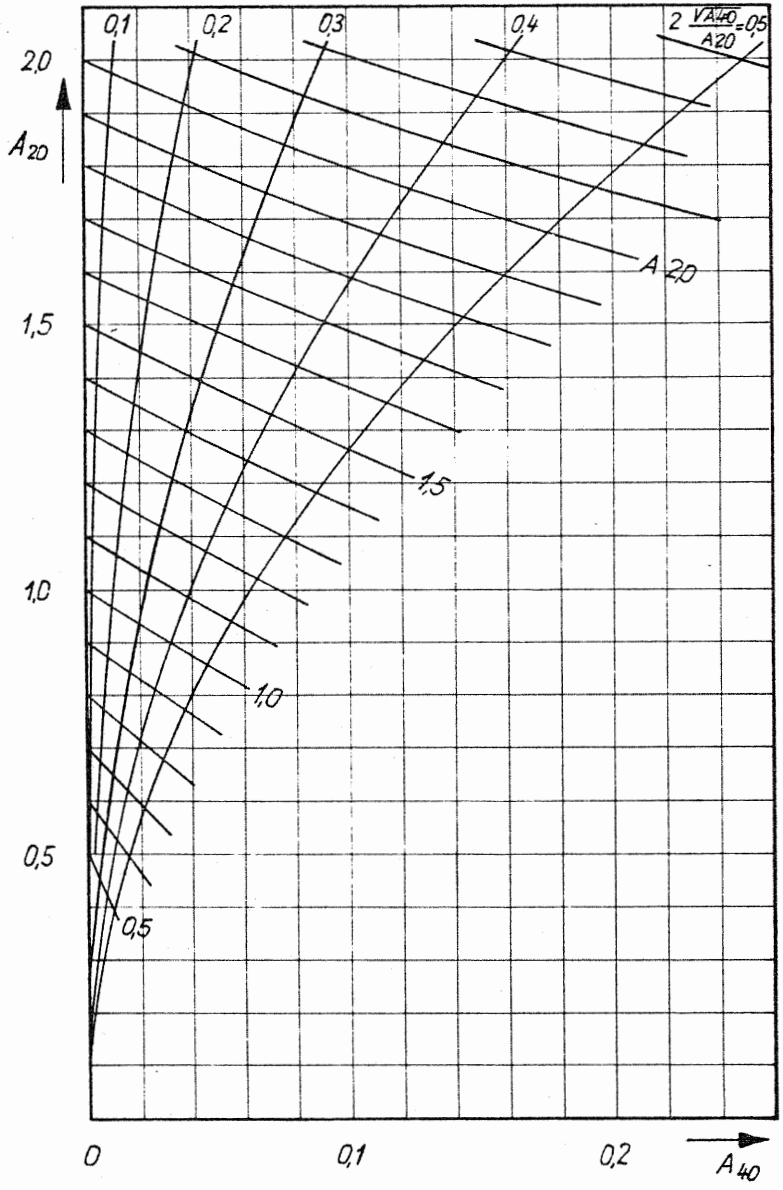

FIG. AII. 3 INVERSE FUNCTION TO FIG. AII. 1: $A_{20} = f(A_2, A_{40})$

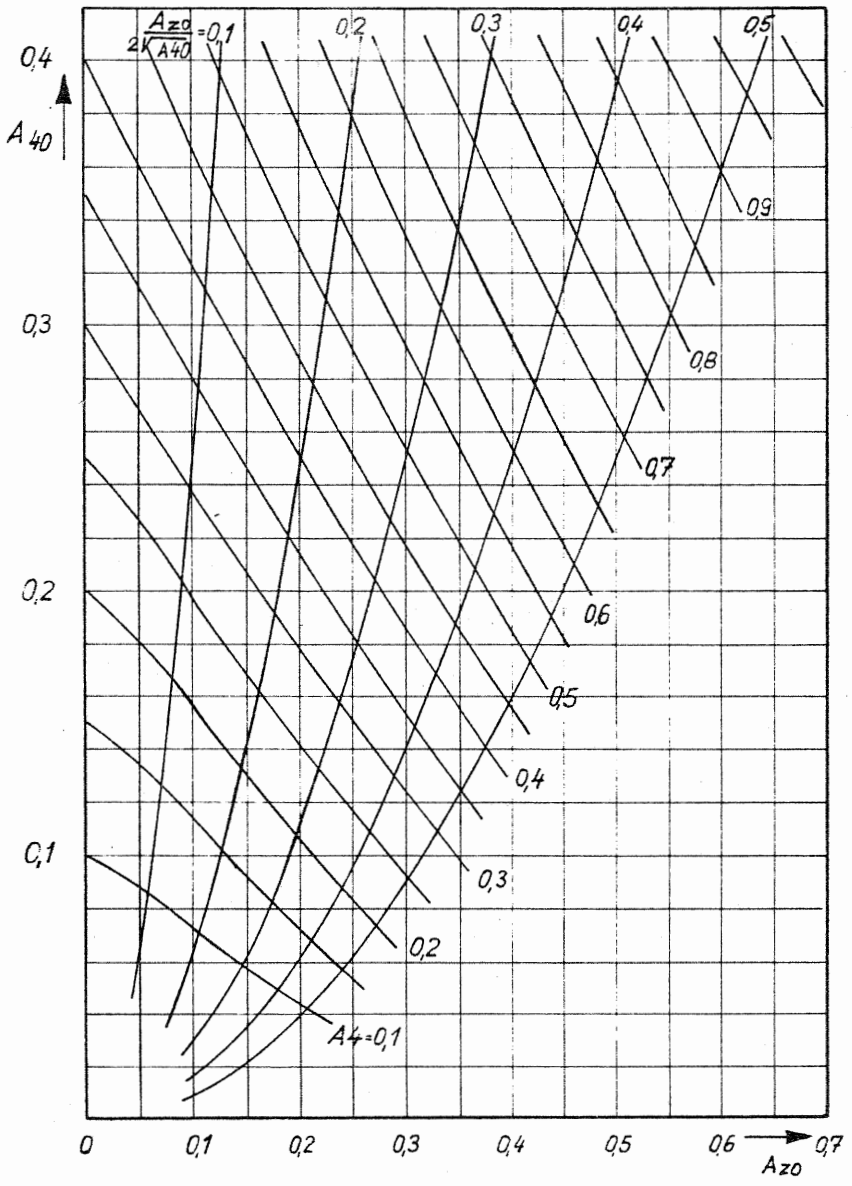

FIG. AII. 4 INVERSE FUNCTION TO FIG. AII. 2: $A_{40} = f(A_4, A_{20})$

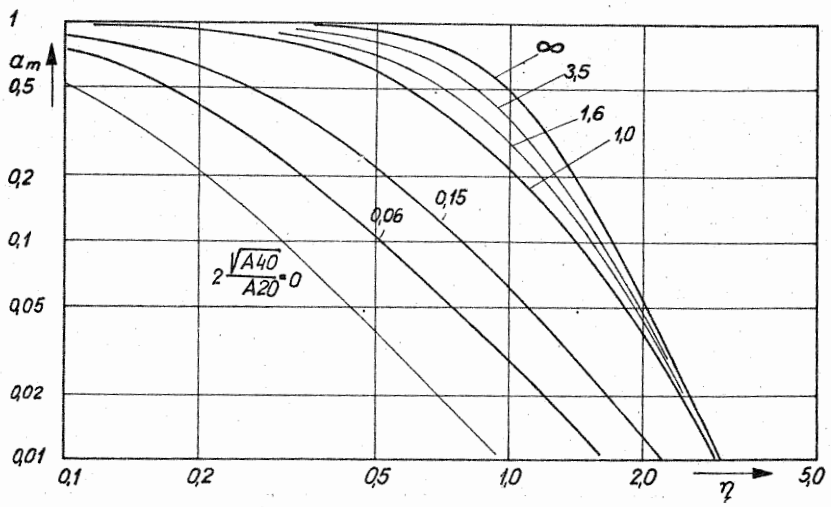

FIG. AIII. 1 ENVELOPES OF NORMALIZED BEAM SPECTRA FOR DIFFERENT RATIOS $2\frac{A_{40}}{A_{20}}$
(NOTE: THE ABSCISA SHOULD BE MULTIPLIED BY 10 IF CURVE FOR $2\frac{A_{40}}{A_{20}} = 0$ IS CONSIDERED).

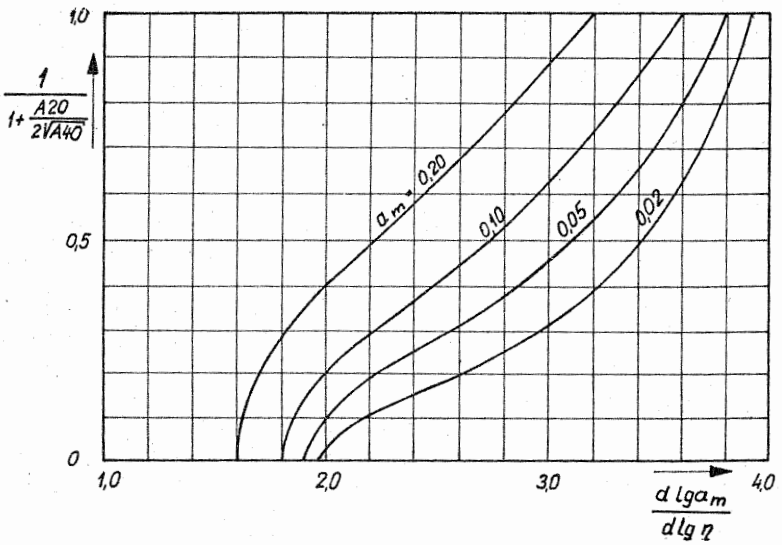

FIG. AIII. 2 CORRELATION BETWEEN SLOPE OF ENVELOPE (SEE FIG. AIII. 1) AND THE RATIO $2\frac{A_{40}}{A_{20}}$

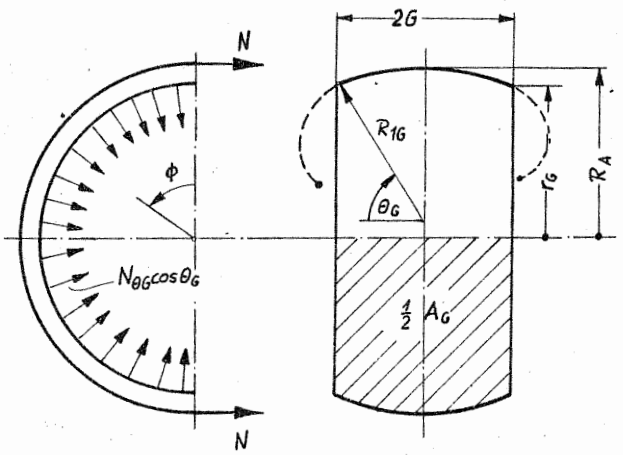

FIG. AIV. 1 BREAKER OF A RADIAL CORD TYRE, AND ITS TENSILE FORCES N, $N_{\theta G}$

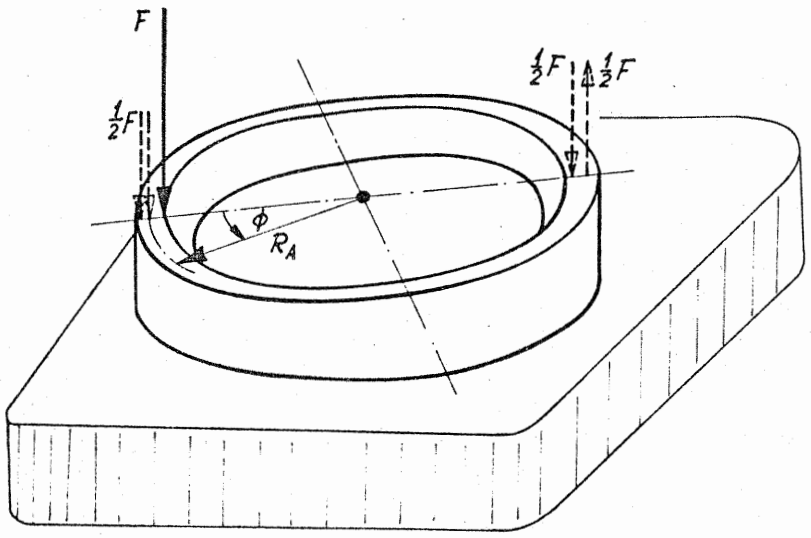

FIG. AV. 1 RIGID HOOP ON ELASTIC FOUNDATION SUBJECTED TO A LATERAL POINT LOAD F (DASHED ARROWS = COMPONENTS OF F)

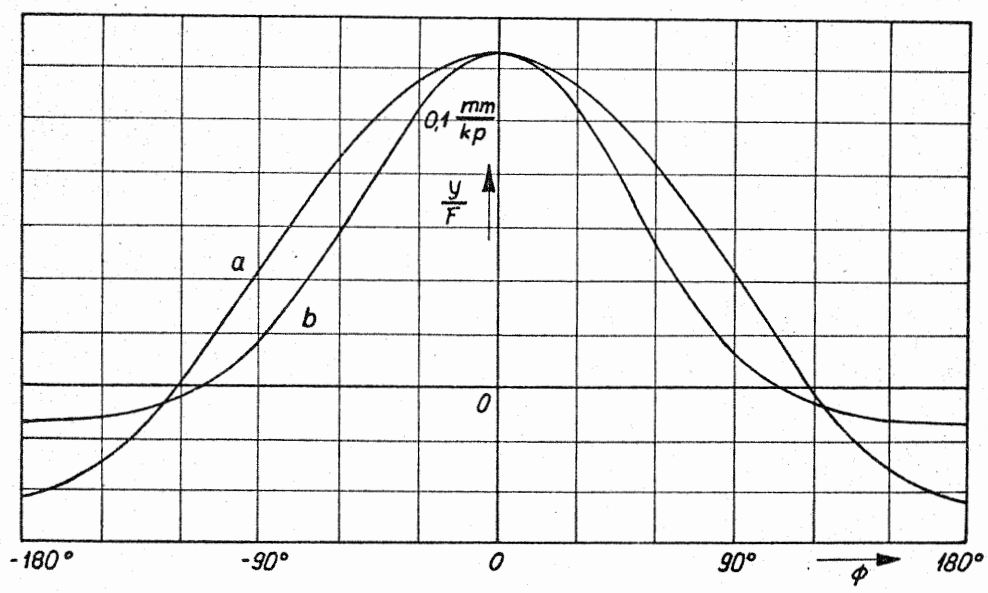

FIG. AV. 2 DEFLECTION LINE OF A RIGID HOOP ON ELASTIC FOUNDATION (CURVE a) COMPARED WITH A BENDING LINE OF A RADIAL CORD TYRE OF TYRE M6.00 - 16X

($p = 1,5 \frac{kp}{cm^2}$, curve b).